LAWRENCE
LIVERMORE
NATIONAL
LABORATORY

UCRL-PROC-202921

Determination of the Crevice Repassivation Potential of Alloy 22 by a Potentiodynamic-Galvanostatic-Potentiostatic Method

Kenneth J. Evans, Lana L. Wong, Raul B. Rebak

March 15, 2004

ASME Pressure Vessel and Piping
San Diego, CA, United States
July 25, 2004 through July 29, 2004

11 March 2004
Paper prepared for presentation to the 2004 American Society of Mechanical Engineers Pressure Vessels and Piping Conference, 25-29 July 2004 in San Diego, CA

Determination of the Crevice Repassivation Potential of Alloy 22 By a Potentiodynamic-Galvanostatic-Potentiostatic Method

Kenneth J. Evans, Lana L. Wong and Raúl B. Rebak
Lawrence Livermore National Laboratory, Livermore, CA 94550

ABSTRACT

Alloy 22 (N06022) is a nickel-based alloy highly resistant to corrosion. In some aggressive conditions of high chloride concentration, temperature and applied potential, Alloy 22 may suffer crevice corrosion, a form of localized corrosion. There are several electrochemical methods that can be used to determine localized corrosion in metallic alloys. One of the most popular for rapid screening is the cyclic potentiodynamic polarization (CPP). This work compares the results obtained by measuring the localized corrosion resistance of Alloy 22 using both CPP and the more cumbersome Tsujikawa-Hisamatsu Electrochemical (THE) method. The electrolytes used were 1 M NaCl and 5 M $CaCl_2$, both at 90°C. Results show that similar repassivation potentials were obtained for Alloy 22 using both methods. That is, in cases where localized corrosion is observed using the fast CPP method, there is no need to use THE method since it takes ten times longer to obtain comparable results in spite that the mode of corrosion attack that results in the tested specimens are different.

INTRODUCTION

Many austenitic alloys such as Alloy 22 (N06022) that rely on the stability of a thin chromium oxide (Cr_2O_3) film for protection against corrosion are prone to crevice corrosion, a form of localized corrosion. Localized corrosion is an insidious type of attack, which forms at discrete sites of the component surface and has a bigger propagation rate than passive corrosion. Both ASTM and NACE International define crevice corrosion as “localized corrosion of a metal surface at, or immediately adjacent to, an area that is shielded from full exposure to the environment because of close proximity between the metal and the surface of another material” [1]

The susceptibility of each chromia forming alloy to localized corrosion depends strongly on the composition of the electrolyte solution, temperature and applied potential. In general, the environment becomes more aggressive with increases in chloride concentration, temperature and applied potential. Not all chromia forming alloys have the same susceptibility to localized corrosion promoted by chloride. Alloys containing increased amount of chromium, molybdenum and nitrogen exhibit superior resistance to this type of attack. Thus, nickel-based Alloy 22 (N06022) has a greater resistance, for

example, to crevice corrosion than iron-based type 316 stainless steel (S31600) since N06022 contains 22% chromium (Cr) and 13% molybdenum (Mo) and S31600 contains 18% Cr and 2.5% Mo.

Alloy 22 or N06022 is nickel-based (Ni) and contains by weight 22% chromium (Cr), 13% molybdenum (Mo), 3% tungsten (W) and approximately 3% iron (Fe). Alloy 22 was commercially designed to resist the most aggressive industrial applications, offering a low general corrosion rate both under oxidizing and reducing conditions [2]. Under oxidizing and acidic conditions Cr exerts its beneficial effect in the alloy. Under reducing conditions the most beneficial alloying elements are Mo and W, which offer a low exchange current for hydrogen discharge [3,4]. Moreover, due to its balanced content in Cr, Mo and W, Alloy 22 is used extensively in hot chloride containing environments where austenitic stainless steels may fail by pitting corrosion and stress corrosion cracking (SCC) [3,4].

Alloy 22 was selected for the fabrication of the outer shell of the high level nuclear waste containers for the Yucca Mountain repository [5,6]. Several papers have been published recently describing the general and localized corrosion resistance of Alloy 22 regarding its application for the nuclear waste containers [6-15]. The Cyclic Potentiodynamic Polarization (CPP) (ASTM G 61) [1] was a popular method used to assess the anodic behavior of Alloy 22 and its response to localized corrosion. Other method that was used to investigate localized corrosion included variations of the technique originally proposed by Tsujikawa and Hisamatsu [16] and later used by other researchers for different alloys [12,17].

There are several methods to determine the susceptibility of an alloy to localized corrosion. These methods can be divided into immersion tests and electrochemical tests (Table 1). In both types of tests the alloys are driven to the limit of resistance to localized corrosion by changing the environmental variables including chloride concentration, temperature and applied potential. That is, each alloy is characterized by, for example, how high a temperature can tolerate without undergoing localized corrosion at a constant chloride concentration and constant applied potential. This is generally assessed as a critical pitting or critical crevice temperature. Table 1 summarizes both types of methods and their significance. There are no universal or single methods for measuring localized corrosion susceptibility of an alloy. Each method provides a different parameter to compare the behavior of one alloy with another in a fixed environment or for one alloy to compare one electrolyte with another. The most popular testing methods were written into ASTM standards but other commonly accepted methods do not have a specific standard (Table 1).

The objective of this research work was to investigate the localized corrosion behavior of Alloy 22 using two electrochemical methods, namely, the cyclic potentiodynamic polarization (CPP –ASTM G 61) and the Tsujikawa-Hisamatsu Electrochemical (THE) method (Table 1) in 1 M NaCl and 5 M $CaCl_2$ solutions at 90°C.

EXPERIMENTAL

Alloy 22 specimens were mainly prepared from 1-inch thick plate. There were several heats of material used in this research. The chemical composition of the most used specimens of Alloy 22 are given in Table 2. The specimens were mainly multiple crevice assemblies (MCA), which were fabricated based on the washer for crevice forming described in ASTM G 48 [1]. The specimen MCA has been described before

[7,9]. The tested surface area of the MCA specimens was approximately 11 cm². All the tested specimens had a finished grinding of abrasive paper number 600 and were degreased in acetone and treated ultrasonically for 5 minutes in de-ionized (DI) water 1 hour prior to testing. Specimens were used in the mill annealed (MA) and in the as-welded (ASW) condition. All of the specimens listed in Tables 3 and 4 were in the MA condition except for the ones with the designation JE, which contained a weld seam. The weld was produced with matching filler metal using Gas Tungsten Arc Welding (GTAW). The welded specimens contained only a narrow (approximately 5 mm wide) band of weld seam across the surface of the specimen that was purposely creviced with the multiple teeth washer.

Electrochemical tests were carried in deaerated 1 M NaCl and 5 M $CaCl_2$ solutions at 90°C. The pH of these solutions was approximately 6.2 and 4, respectively. Nitrogen (N_2) was purged through the solution at a flow rate of 100cc/min for 24 hours while the corrosion potential (E_{corr}) was monitored. Nitrogen bubbling was carried throughout all the electrochemical tests. The electrochemical tests were conducted in a one-liter, three-electrode, borosilicate glass flask (ASTM G 5) [1]. A water-cooled condenser combined with a water trap was used to maintain solution concentration and controlled atmosphere. The temperature of the solution was controlled by immersing the cell in a thermostatisized silicone oil bath. All the tests were carried at ambient pressure. The reference electrode was saturated silver chloride (SSC) electrode, which has a potential of 199 mV more positive than the standard hydrogen electrode (SHE). The reference electrode was connected to the solution through a water-jacketed Luggin probe so that the electrode was maintained at near ambient temperature. The counter electrode was a flag (36 cm^2) of platinum foil spot-welded to a platinum wire. All the potentials in this paper are reported in the SSC scale.

Basically the test sequence for each specimen consisted of three parts: (1) E_{corr} evolution as a function of time for 24 h, (2) Polarization Resistance (ASTM G 59) three subsequent times and (3) A larger anodic polarization to determine susceptibility to crevice corrosion. The larger anodic polarization was conducted using two methods: (i) Cyclic Potentiodynamic Polarization (CPP) method and (ii) Tsujikawa-Hisamatsu Electrochemical (THE) method.

Polarization Resistance (ASTM G 59): Corrosion rates (CR) were obtained using the polarization resistance method (ASTM G 59) [1]. Each one of these tests lasts approximately four minutes. An initial potential of 20 mV below the corrosion potential (E_{corr}) was ramped to a final potential of 20 mV above E_{corr} at a rate of 0.167 mV/s. Linear fits were constrained to the potential range of 10 mV below E_{corr} to 10 mV above E_{corr}. The Tafel constants, β_a and β_c, were assumed to be $\pm$ 0.12 V/decade. Corrosion rates were calculated using Equation 1

$$CR(nm/yr) = k\frac{i_{corr}}{\rho}EW \qquad \textbf{(1)}$$

Where k is a conversion factor (3.27 x 10^9 $nm \cdot g \cdot A^{-1} \cdot cm^{-1} \cdot yr^{-1}$), i_{corr} is the measured corrosion current density in A/cm^2, EW is the equivalent weight, and ρ is the density of Alloy 22 (8.69 g/cm^3). Assuming an equivalent dissolution of the major alloying elements as Ni^{2+}, Cr^{3+}, Mo^{6+}, Fe^{2+}, and W^{6+}, the EW for Alloy 22 is 23.28 (ASTM G 102) [1].

Cyclic Potentiodynamic Polarization - CPP (ASTM G 61): One of the tests to assess the susceptibility of Alloy 22 to localized corrosion and passive stability was the cyclic potentiodynamic polarization technique, CPP (ASTM G 61) [1]. The potential scan was started 150 mV below E_{corr} at a set scan rate of 0.167 mV/s. The scan direction was reversed when the current density reached 5 mA/cm^2 in the forward scan. Depending on the range of applied potentials, each CPP test could last between 1 h and 3 h.

Tsujikawa-Hisamatsu Electrochemical - THE: The second test used to assess the susceptibility of Alloy 22 to localized corrosion and passive stability was the Tsujikawa-Hisamatsu Electrochemical test, which does not have still a standard even though it was introduced to the corrosion community about 20 years ago [16]. The potential scan was started 150 mV below E_{corr} at a set potentiodynamic scan rate of 0.167 mV/s. Once the current density reached a predetermined value (for example 20 µA/cm² or 2 µA/cm²), the controlling mode was switched from potentiodynamic to galvanostatic and the predetermined current density is applied for usually 2 h. Some tests were conducted holding a galvanostatic treatment for 4 h and 8 h. The resulting potential at the end of the galvanostatic treatment was recorded. After the galvanostatic step, the treatment was switched to a potentiostatic mode. The potentiostatic steps were applied for 2 h starting at the potential recorded at the end of the galvanostatic treatment and applying as many steps as necessary until crevice repassivation was achieved. Each subsequent potentiostatic step was 10 mV lower that the previous step. Generally 10 steps (or a total of 100 mV) were necessary to achieve repassivation of an active crevice-corrosion. The repassivation potential is determined as the potential for which the current density decreases as a function of time in the period of treatment of 2 h. Depending of the applied time and number of potentiostatic steps, each THE test could last between 24 h and 30 h.

After the CPP and THE tests, the specimens were examined in an optical stereomicroscope at a magnification of 20 times to establish the mode and location of the attack. A few specimens were also studied using a scanning electron microscope (SEM).

RESULTS AND DISCUSSION

The Corrosion Potential (E_{corr})

Figure 1 shows the corrosion potential (E_{corr}) of individual MCA samples of Alloy 22 in 5 M $CaCl_2$ and 1 M NaCl at 90°C as a function of the immersion time. The total immersion time was 24 h or 86,400 s. Figure 1 shows that, after an initial transient period of approximately 5 h, E_{corr} remained approximately constant as the time increased. Figure 1 also shows that E_{corr} was higher in the $CaCl_2$ brine than in the NaCl brine. The average E_{corr} for Alloy 22 in 5 M $CaCl_2$ (10 M Cl^-) was –327 mV (SSC) and in 1 M NaCl (1 M Cl^-) was –508 mV (SSC), a difference of 181 mV between both solutions (Tables 3 and 4). The higher E_{corr} in the $CaCl_2$ brine could be a result of the pH of the solution. The ambient pH of 5 M $CaCl_2$ solution was approximately 4 while the pH of the 1 M NaCl solution was approximately 6.2. The slope in the Nernst equation at 90°C is –0.072pH (V), therefore, the difference of pH between both solutions would account for 158 mV in potential difference between these two solutions. This number is close to the actual difference between average E_{corr} values reported above and in Tables 3 and 4. In each solution, the E_{corr} of MA and ASW specimens were the same. It was reported before that the E_{corr} of Alloy 22 in deaerated concentrated $CaCl_2$ brines was practically

independent of the temperature and approximately –360 mV (SSC) [9]. In aerated 5 M $CaCl_2$ brine at 120°C, E_{corr} was –130 mV (SSC) [18].

Polarization Resistance and Corrosion Rate (CR)

Tables 3 and 4 show the corrosion rates (CR) of MA and ASW Alloy 22 in 1 M NaCl and 5 M $CaCl_2$ at 90°C, respectively. The average corrosion rates values in both solutions was low and practically the same, in the order of 1.7 µm/year. The uniform corrosion rate of nickel alloys in near neutral chloride containing solutions is in general very low. Immersion tests for 96 h in boiling 4 M NaCl and synthetic seawater showed that the corrosion rate of nickel alloys N06600, N06825, N06455 and N10276 was below 0.1 mpy (2.5 µm/y) [19].

Cyclic Potentiodynamic Polarizations (CPP)

Figure 2 shows the cyclic potentiodynamic polarization for a MA Alloy 22 specimen in deaerated 1 M NaCl at 90°C. The material did not show a classical passive region with the current density totally independent of applied potential. The current density increased gradually as the applied potential increased until a pseudo breakdown was observed at a potential higher than 0.2 V (SSC). The highest polarization was near 1 V (SSC) (Figure 2). The reverse polarization showed a delayed hysteresis, suggesting the nucleation and growth of crevice corrosion during the reverse scan. After the tests, all the examined specimens in Table 3 showed crevice corrosion under the crevice formers. When welded specimens were tested in 1 M NaCl solution (Table 3), crevice corrosion formed both in the base metal and in the welded seam. In general, there were more areas of attack in the base metal than in the weld seam, but this could only be a result of having a higher surface of exposed base metal than of weld seam to the crevice former washer. Characteristic potential values from Figure 2 and other tested specimens are listed in Table 3.

Figure 3 shows the cyclic potentiodynamic polarization for a welded Alloy 22 specimen in deaerated 5 M $CaCl_2$ at 90°C. The material showed a classical passive region with the current density practically independent of applied potential until the breakdown potential just above 0 V (SSC). Then, the current density increased abruptly and the reverse polarization showed a clear hysteresis, suggesting the nucleation and growth of localized corrosion at the point of potential breakdown. After the tests, the examined specimen showed that localized attack started at the crevice formers and progressed outwards towards the metal exposed boldly to the solution. The attack was related to the presence of the crevice former but did not propagate below the crevice former. This has been reported before [9]. The highest polarization in Figure 3 was less than 0.2 V (SSC). The localized attack in welded specimens (Table 4) occurred equally in the base metal and in the weld seam. Characteristic potential values from Figure 3 and other tested specimens are listed in Table 4.

Tsujikawa Hisamatsu Electrochemical (THE)

Figures 4 and 5 show the results from THE tests for Alloy 22 MCA specimens in 1 M NaCl and 5 M $CaCl_2$ at 90°C, respectively. The repassivation potentials (ER,CREV) [16,17] for the tests in Figures 4 and 5 and other specimens are listed in Tables 3 and 4. The current density curve in Figure 4 (1 M NaCl) was more erratic than the current

density curve in Figure 5 (5 M $CaCl_2$). This was also characteristic for other tests reported in Tables 3 and 4 in the same solutions. That is, the ER,CREV in $CaCl_2$ solutions was easier to determine, since it was clearer when the current density did not increase as a function of time. After the THE tests, all of the tested specimens, both in NaCl and $CaCl_2$ brines showed crevice corrosion under the crevice former washers.

Table 4 also shows the results from a series of tests in 5 M $CaCl_2$ in which the galvanostatic hold of 2 µA/cm²in THE tests was maintained for 2 h, 4 h and 8 h and when a current density of 20 µA/cm² was maintained for 8 h. In each of these cases the amount of charge for dissolution or enlargement of the crevice corroded area was different; however, data in Table 4 shows that the ER,CREV was the same and approximately –130 mV. That is, under the tested conditions, the repassivation potential was not a function of the amount of charged passed through the specimens. This has been reported before (7)

Type of Localized Attack as a function of Test Method

The nature of the localized attack changed with the testing method. In 1 M NaCl solution, the attack in the specimens tested using CPP was deeper at the edges of the crevice formers and did not propagate horizontally extensively below each crevice former (Figures 6 and 7). On the other hand, using THE method, the crevice corrosion attack was of the same depth throughout and with an almost full penetration horizontally below the crevice former (Figures 8 and 9). In both cases, in the crevice-corroded area, the attack was intergranular and crystallographic, that is, grains and metal planes within grains were discernible.

In 5 M $CaCl_2$ solution, when tested using CPP most of the attack occurred outside the crevice former (Figures 10 and 11). The localized corrosion started at the washer-metal interface but then progressed in a massive way towards the outside of the specimen, mostly following gravitational directions. When using THE method, the specimen suffered crevice corrosion under the crevice former (Figures 12 and 13). The attack started at the washer-metal interface and progressed underneath the washer. The depth of attack was not uniform since it was deeper towards the perimeter of the washer (Figure 13). In both cases, in the crevice-corroded area of the base metal, the attack was intergranular and crystallographic, that is, grains and metal planes within grains were discernible. Also, following both testing methods, the extent of attack was similar in base metal and in the weld seam (Figures 11 and 12).

The fact that the mode of attack is different using CPP or THE methods could be tracked to the way the anodic current is applied to the specimen. Using the CPP method, the potential is continuously raised in a short time (sometimes less than 1 h) to relatively high values until a current density of 5 mA/cm² is reached. This produces a highly aggressive condition that generates massive dissolution of the metal in 5 M $CaCl_2$ and localized attack along the perimeter of the washer in 1 M NaCl (Figures 5, 7, 10 and 11). By applying a high current density of up to 5 mA/cm² the material is driven into transpassivity in the boldly exposed surfaces in the case of 1 M NaCl and to massive localized dissolution in the case of 5 M $CaCl_2$. However, when THE method is used, the current density that is applied is approximately 1000 times lower (20 or 2 µA/cm²) for longer periods of time, thus allowing for crevice corrosion to nucleate and propagate under the crevice former where a solution more aggressive than the bulk forms (Figures 8, 9, 12 and 13).

Parameters from the Anodic Polarization Curves

In the cyclic potentiodynamic polarization (CPP) curves (Figures 2 and 3) there are several typical potentials. One of these potentials is the corrosion potential or the potential for which the applied cathodic and anodic currents are the same. Another typical potential is the breakdown potential for which the current density increases significantly and rather rapidly above the passive current density. The passive current density is defined as the region of potentials in which the current density is not highly dependent on the applied potential. Figures 2 and 3 show arrows indicating the values of current density of 20 $\mu A/cm^2$ and 200 $\mu A/cm^2$ for the forward scan and 10 $\mu A/cm^2$ and 1 $\mu A/cm^2$ for the reverse scan. The values of potential for which the above-mentioned current densities are reached are called respectively E20, E200, ER10 and ER1. The values E20 and E200 represent breakdown potentials and the values ER10 and ER1 represent repassivation potentials. That is, in the forward scan, when the current density reaches for example 200 $\mu A/cm^2$ the passive behavior of the alloy does not longer exists and when the current density in the reverse scan has reached 1 $\mu A/cm^2$, it can be considered that the alloy has regained its passive behavior prior to the breakdown. The values of these four parameters are listed in Table 3 and 4. Another parameter of interest is the repassivation potential determined as the intersection of the reverse scan with the forward scan. This is call ERCO or repassivation potential cross over (Figures 2-3 and Tables 3-4).

In the current density/potential representations resulting from THE tests, the ER,CREV value is obtained. The ER,CREV is the crevice repassivation potential as defined by the originators of this testing method [16,17]. The values of ER,CREV are also shown in Figures 4-5 and listed in Tables 3 and 4. All the six listed parameters allow comparison among test results without the clutter of superimposing many current-potential curves.

Figure 14 shows the values of E_{corr}, E20, E200, ER10, ER1, ERCO and ER,CREV for Alloy 22 in 1 M NaCl solution at 90°C from Table 3. Figure 14 shows that the breakdown potentials (E20 and E200) are approximately 800 mV more anodic than E_{corr}; however, the repassivation potentials (e.g. ER1) are approximately 400 mV more anodic than E_{corr}. Figure 14 and Table 3 also show that the repassivation potentials have practically the same values defined by different parameters in the CPP method (ER10, ER1 and ERCO) and also by the THE method (ER,CREV). The repassivation potentials defined as ER1 seem to be the most conservative (lowest values) and having the least amount of scatter in the values (Table 3). The values of ER1 are also easier to obtain from the CPP curves than the ERCO values. The average values of repassivation potentials defined as ER1, ERCO and ER,CREV are only a maximum of 40 mV apart from each other (Figure 14, Table 3). This shows that the use of CPP is a preferable technique for testing since it is faster and gives more information than THE technique.

Figure 15 shows the values of E_{corr}, E20, E200, ER10, ER1, ERCO and ER,CREV for Alloy 22 in 5 M $CaCl_2$ solution at 90°C from Table 4. Figure 15 shows that the breakdown potentials are approximately 400 mV more anodic than E_{corr}; however, the repassivation potentials are approximately 250 mV more anodic than E_{corr}. Figure 15 and Table 4 also show that the repassivation potentials have practically the same values defined by different parameters in the CPP method (ER10, ER1 and ERCO) and also by the THE method (ER,CREV). The repassivation potentials defined as ER1 and ER,CREV seem to have the smallest standard deviation (Table 4 and Figure 15). Figure 15 and Table 4 also show that the ER1 parameter has lower standard deviation than the ERCO parameter. Moreover, ER1 is easier and faster to determine from CPP curves than ERCO.

The most conservative (lowest values) repassivation potential is the one defined as ER1. However, the average values of repassivation potentials defined as ER1, ERCO and ER,CREV are only a maximum of 50 mV apart from each other (Figure 15, Table 4).

Results from Figures 14-15 and Tables 3-4 show that THE method does not provide additional information over CPP regarding the resistance of Alloy 22 to localized corrosion under the tested conditions. The time involved to perform THE tests is ten times longer than the time to perform CPP tests. It is not discarded that THE method could provide additional information regarding the resistance of Alloy 22 to localized corrosion when using the CPP test the alloy does not undergo localized corrosion. For example, in instances when using CPP, only transpassivity of the boldly exposed surface is observed.

Table 3 shows that the ER,CREV of welded Alloy 22 in 1 M Cl^- solutions at 90°C was similar regardless if the solution was prepared using NaCl, $CaCl_2$, $MgCl_2$ or KCl salt. The values of ER,CREV ranged from -72 mV (SSC) for 1 M NaCl solution to –90 mV (SSC) for the 1 M KCl solution. This data is preliminary and may need to be investigated further.

Figure 16 shows comparatively the average values of all the parameters in Figures 14-15 for both 1 M NaCl and 5 M $CaCl_2$ solutions. As anticipated, Figure 16 shows that the 5 M $CaCl_2$ solution was more aggressive towards the resistance of Alloy 22 to localized corrosion than the 1 M NaCl solution at the same temperature. That is, Alloy 22 has lower breakdown and repassivation potentials in 5 M $CaCl_2$ than in 1 M NaCl.

CONCLUSIONS

1. The Cyclic Potentiodynamic Polarization (CPP) method provided information on the resistance of Alloy 22 to localized corrosion after 3 h of testing. The obtained values of breakdown potential and repassivation potential are highly objective.

2. The Tsujikawa-Hisamatsu Electrochemical (THE) method provided only the value of repassivation potential after 30 h of testing. The values could be subjective.

3. The mode of localized corrosion observed in the tested specimens varied when using CPP or THE methods. However, the repassivation potentials remained the same.

4. The values of repassivation potentials obtained using CPP and THE, differed by a maximum of 50 mV in both of the tested solutions.

5. The weld seam and the base metal showed comparable resistance to localized corrosion.

6. The amount of passed charge during anodic polarization to grow the localized corrosion did not influence the value of repassivation potential

7. Whenever localized corrosion is observed using the CPP method, THE method does not provide additional information on the values of repassivation potential.

ACKNOWLEDGMENTS

This work was performed under the auspices of the U. S. Department of Energy by the University of California Lawrence Livermore National Laboratory under contract N° W-7405-Eng-48. The work was supported by the Yucca Mountain Project, which is part of the DOE Office of Civilian Radioactive Waste Management (OCRWM).

REFERENCES

1. ASTM International, Volume 03.02, Standards G 5, G 15, G 48, G 59, G 61, G 102 (ASTM International, 2003: West Conshohocken, PA).
2. Haynes International, "Hastelloy C-22 Alloy", Brochure H-2019E (Haynes International, 1997: Kokomo, IN).
3. R. B. Rebak in Corrosion and Environmental Degradation, Volume II, p. 69, Wiley-VCH, Weinheim, Germany (2000).
4. R. B. Rebak and P. Crook, *Advanced Materials and Processes*, February 2000.
5. Yucca Mountain Science and Engineering Report, U. S. Department of Energy, Office of Civilian Radioactive Waste Management, DOE/RW-0539, Las Vegas, NV, May 2001.
6. G. M. Gordon, Corrosion, 58, 811 (2002).
7. B. A. Kehler, G. O. Ilevbare and J. R. Scully, Corrosion, 1042 (2001).
8. K. J. Evans and R. B. Rebak in Corrosion Science – A Retrospective and Current Status in Honor of Robert P. Frankenthal, PV 2002-13, p. 344-354 (The Electrochemical Society, 2002: Pennington, NJ).
9. K. J. Evans, S. D. Day, G. O. Ilevbare, M. T. Whalen, K. J. King, G. A. Hust, L. L. Wong, J. C. Estill and R. B. Rebak, PVP-Vol. 467, Transportation, Storage and Disposal of Radioactive Materials – 2003, p. 55 (ASME, 2003: New York, NY).
10. S. D. Day, K. J. Evans and G. O. Ilevbare, in "Critical Factors in Localized Corrosion IV", PV 2002-24, p. 534 (The Electrochemical Society, 2003: Pennington, NJ).
11. D. S. Dunn, G. A. Cragnolino, and N. Sridhar, in Scientific Basis for Nuclear Waste Management XXIV, Vol. 608, p 89 (Materials Research Society, 2000: Warrendale, PA).
12. G. A. Cragnolino, D. S. Dunn and Y.-M. Pan, in Scientific Basis for Nuclear Waste Management XXV, Vol. 713, p 53 (Materials Research Society, 2002: Warrendale, PA).
13. V. Jain, D. Dunn, N. Sridhar and L. Yang, Corrosion/2003, Paper 03690 (NACE International, 2003: Houston, TX).
14. D. S. Dunn, L. Yang, Y. – M. Pan and G. A. Cragnolino, Corrosion/2003, Paper 03697 (NACE International, 2003: Houston, TX).
15. N. S. Meck, P. Crook, S. D. Day and R. B. Rebak, Corrosion/2003, Paper 03682 (NACE International, 2003: Houston, TX).
16. S. Tsujikawa and Y. Hisamatsu, Corr. Eng. Japan, 29, 37 (1980).
17. M. Akashi, G. Nakayama and T. Fukuda, Corrosion/98, Paper 98158 (NACE International, 1998: Houston, TX).
18. J. C. Estill, G. A. Hust and R. B. Rebak, Corrosion/2003, Paper 03688 (NACE International, 2003: Houston, TX).
19. Database from Haynes International Inc. (Kokomo, IN).

Table 1
Testing Methods to Determine Localized Corrosion of
Chromia Forming Alloys (Fe, Ni and Co alloys)

Test	Standard	Fixed Variables	Obtained Parameter
Immersion			
6% Ferric Chloride	ASTM G 48	Electrolyte, Potential	Critical Pitting and Critical Crevice Temperature (CPT and CCT)
Sea Water	ASTM G 78	Electrolyte, Temperature, Potential	Various, Mainly for alloy comparison
Electrochemical			
Cyclic Potentiodynamic Polarization (CPP)	ASTM G 61	Temperature, Electrolyte	Critical Potentials (Breakdown e.g. E20, Repassivation e.g. ER1)
Potentiostatic with temperature increase at constant rate	ASTM G 150	Potential, Electrolyte	Critical Pitting Temperature (CPT)
Sequential Potentiodynamic + Galvanostatic + Potentiostatic (A)	No Standard	Electrolyte, Temperature	Crevice Repassivation Potential (ER,CREV)
Potentiostatic	No Standard	Electrolyte, Temperature	Crevice Initiation Potential, Time or Growth Rate

(A) Also known as the Tsujikawa Hisamatsu Electrochemical (THE) method

Table 2
Chemical Composition in weight percent of the Materials Used for testing

Specimens/Element	Ni	Cr	Mo	W	Fe	Others
Nominal ASTM B 575	50-62	20-22.5	12.5-14.5	2.5-3.5	2-6	2.5Co-0.5Mn-0.35V (A)
DEA Heat 2277-1-3265	~57	21.2	12.9	2.5-3.5	3.9	0.7Co-0.25Mn-0.17V
JE Base Heat 059902LL1	59.56	20.38	13.82	2.64	2.85	0.17V-0.16Mn
JE1634-1651 Weld Wire	59.31	20.44	14.16	3.07	2.2	0.21Mn-0.15Cu-

(A) Maximum

Table 3: Results from Electrochemical Tests
Comparison Between Cyclic Potentiodynamic Polarization (CPP) and Tsujikawa-Hisamatsu Electrochemical (THE) Methods for Determining Susceptibility to Crevice Corrosion of Alloy 22 (N06022) in 1 M NaCl and other 1 M Cl^- Solutions at 90°C.
Crevice corrosion was observed in all the Specimens.

Specimen ID	Type of Specimen and Material	E_{corr}, 24 h (mV, SSC)	Corrosion Rates (µm/year)	E20 CPP (mV, SSC)	E200 CPP (mV, SSC)	ER10 CPP (mV, SSC)	ER1 CPP (mV, SSC)	ERCO CPP (mV, SSC)	ER, CREV THE (mV, SSC)
SRG01	PCA, Base	-578	1.23, 1, 0.62	302	527	-9	-72	-79	NA
SRG13	PCA, Base	-577	1.69, 1.53, 1.29	306	513	-6	-76	-80	NA
DEA3129	MCA, Base	-298	0.74, 0.95, 0.63	234	674	25	-51	-24	NA
DEA3130	MCA, Base	-237	0.93, 1.2, 0.68	291	582	-14	-75	-67	NA
DEA3262	MCA, Base	-571	1.93, 1.66, 1.36	386	635	30	-94	-53	NA
DEA3263	MCA, Base	-594	2.55, 2.40, 1.29	315	612	20	-99	-54	NA
DEA3269 (A)	MCA, Base	-548	1.21, 1.04, 0.61	271	631	-10	-66	-66	NA
DEA3131	MCA, Base	-604	3.07, 2.44, 1.39	NA	NA	NA	NA	NA	-23
SRG02	PCA, Base	-600	2.31, 1.96, 1.45	NA	NA	NA	NA	NA	49
DEA3132	MCA, Base	-513	3.26, 3.05, 2.89	NA	NA	NA	NA	NA	-20
SRG03	PCA, Base	-577	2.96, 2.34, 1.87	NA	NA	NA	NA	NA	<-10
DEA3133	MCA, Base	-594	NA	NA	NA	NA	NA	NA	-42
DEA3134	MCA, Base	-605	NA	NA	NA	NA	NA	NA	-30
DEA3135	MCA, Base	-333	NA	NA	NA	NA	NA	NA	-33
DEA3136	MCA, Base	-386	NA	NA	NA	NA	NA	NA	-36
JE1639 (B)	MCA, Welded	-260	NA	NA	NA	NA	NA	NA	-72
JE1636 (B) (C)	MCA, Welded	-481	NA	NA	NA	NA	NA	NA	-88
JE1637 (B) (D)	MCA, Welded	-445	NA	NA	NA	NA	NA	NA	-88
JE1638 (B) (E)	MCA, Welded	-497	NA	NA	NA	NA	NA	NA	-90
Ave.±σ (F)	NA	-508 ± 122	1.68 ± 0.79	301 ± 43	596 ± 55	5 ± 18	-76 ± 15	-60 ± 18	-35 ± 17

NA = Not Available or Not Applicable, (A) 1.25 M NaCl, (B) Galvanostatic Current at 2 µA/cm², (C) Tested in 0.5 M $CaCl_2$ Solution, (D) Tested in 0.5 M $MgCl_2$ Solution, (E) Tested in 1 M KCl Solution, (F) For NaCl Solutions Only.
PCP = Potentiodynamic Cyclic Polarization, THE = Tsujikawa Hisamatsu Electrochemical

Table 4
Results from Electrochemical Tests
Comparison Between Cyclic Potentiodynamic Polarization (CPP) and Tsujikawa-Hisamatsu Electrochemical (THE) Methods for Determining Susceptibility to Crevice Corrosion of Alloy 22 (N06022) in 5 M $CaCl_2$ Solutions at 90°C.
All the Tested Specimens Suffered Crevice Corrosion.

Specimen ID	Type of Specimen and Material	$E_{corr,}$ 24 h (mV, SSC)	Corrosion Rates (µm/year)	E20 CPP (mV, SSC)	E200 CPP (mV, SSC)	ER10 CPP (mV, SSC)	ER1 CPP (mV, SSC)	ERCO CPP (mV, SSC)	ER, CREV THE (mV, SSC)
JE1607	MCA, Welded	-345	2.22, 2.11, 1.93	NA	NA	NA	NA	NA	-129
JE1608	MCA, Welded	-310	2.49, 2.16, 2.05	NA	NA	NA	NA	NA	-127
JE1628 (A)	MCA, Welded	-344	1.66, 1.93, 1.53	NA	NA	NA	NA	NA	-131
JE1629 (B)	MCA, Welded	-339	1.66, 1.51, 1.33	NA	NA	NA	NA	NA	-125
JE1630 (C)	MCA, Welded	-340	1.84, 1.65, 1.46	NA	NA	NA	NA	NA	-133
JE1632 (D)	MCA, Welded	-337	1.91, 1.25, 1.70	NA	NA	NA	NA	NA	-133
DEA3216 (E)	MCA, Base	-349	NA	105	128	-136	-182	-200	NA
DEA3217 (E)	MCA, Base	-312	NA	47	130	-115	-174	-129	NA
DEA3218 (E)	MCA, Base	-368	NA	-49	151	-147	-193	-141	NA
DEA3219 (E)	MCA, Base	-342	NA	146	175	-113	-180	-148	NA
JE0037 (E)	MCA, Welded	-253	NA	152	160	-140	-184	-195	NA
JE0038 (E)	MCA, Welded	-313	NA	129	175	-138	-175	-163	NA
JE0039 (E)	MCA, Welded	-286	NA	114	139	-131	-181	-175	NA
JE1635	MCA, Welded	-335	1.57, 1.42, 1.40	71	88	-142	-162	-164	NA
Ave.±σ (F)	NA	-327 ± 28	1.75 ± 0.32	89 ± 62	143 ± 27	-133 ± 12	-179 ± 8	-164 ± 23	-130 ± 3

(A) Galvanostatic step in THE method at 2 µA/cm² for 2 h, (B) at 2 µA/cm² for 4 h and (C) at 2 µA/cm² for 8 h, (D) at 20 µA/cm² for 8 h. (E) Data Previously Published (9).

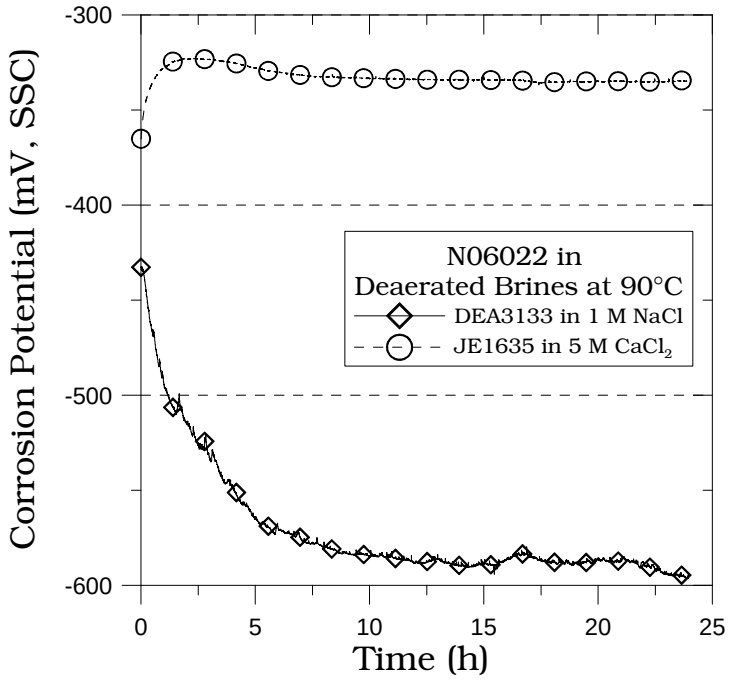

Figure 1: Corrosion Potential Evolution for MCA Alloy 22 samples in two chloride brines at 90°C.

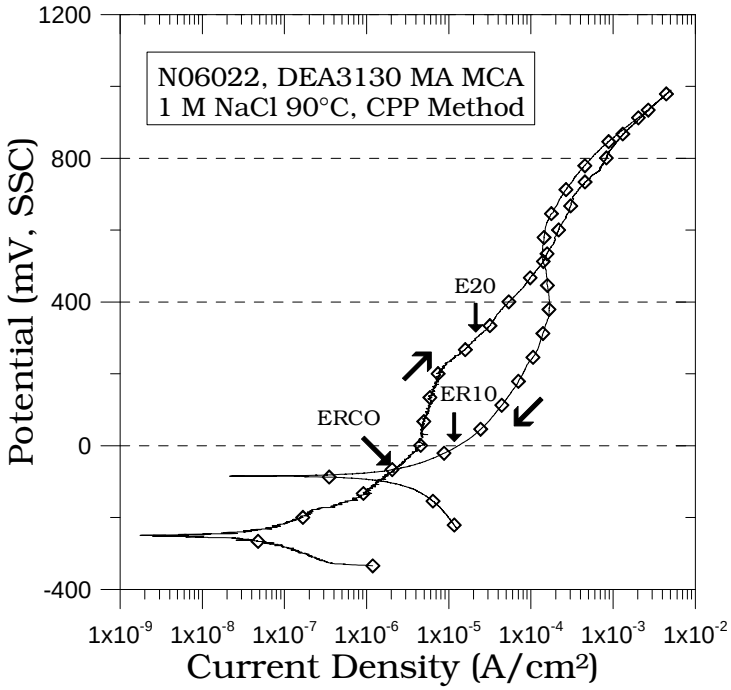

Figure 2: CPP for Alloy 22 in 1 M NaCl
Crevice Corrosion was observed in the specimen after the test

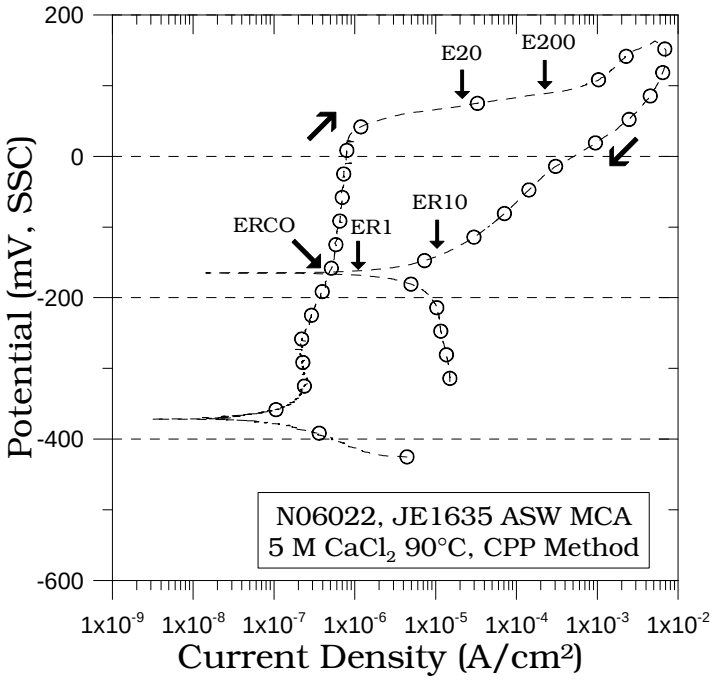

Figure 3: CPP for Alloy 22 in 5 M $CaCl_2$.
Localized Corrosion was observed in the specimen after the test

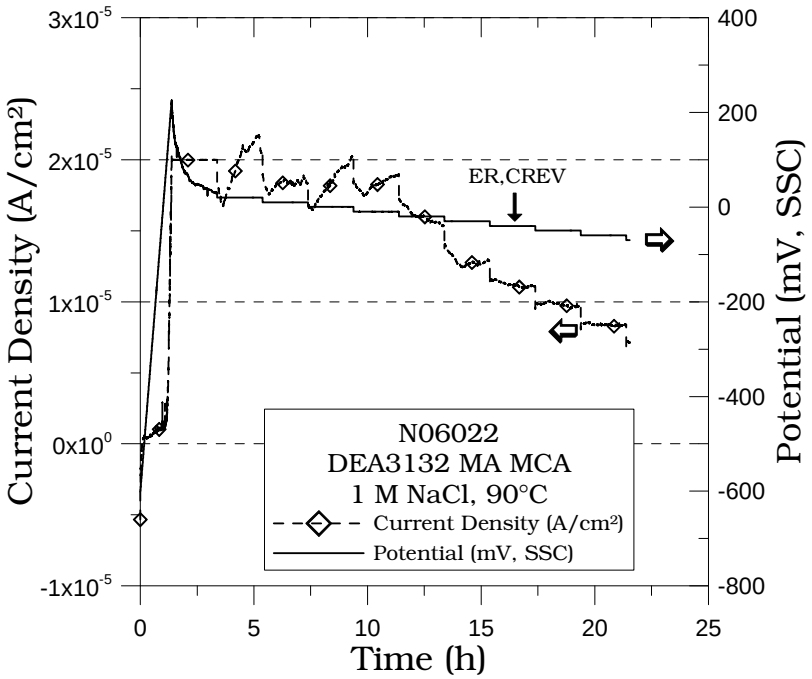

Figure 4: Results from THE tests in 1 M NaCl at 90°C.
The current density curve is more erratic than in Figure 5.

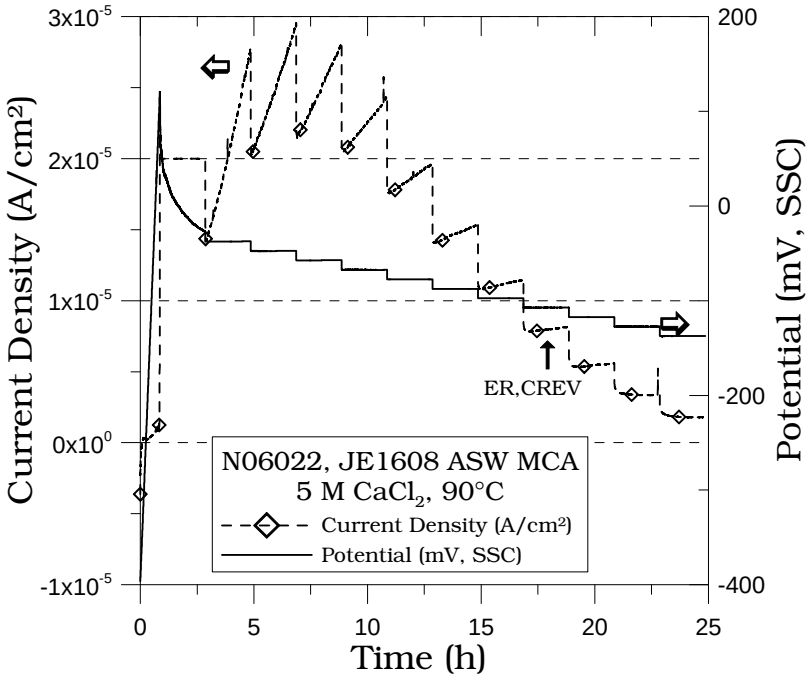

Figure 5: Results from THE tests in 5 M $CaCl_2$ at 90°C. The current density curve is smooth compared to Figure 4.

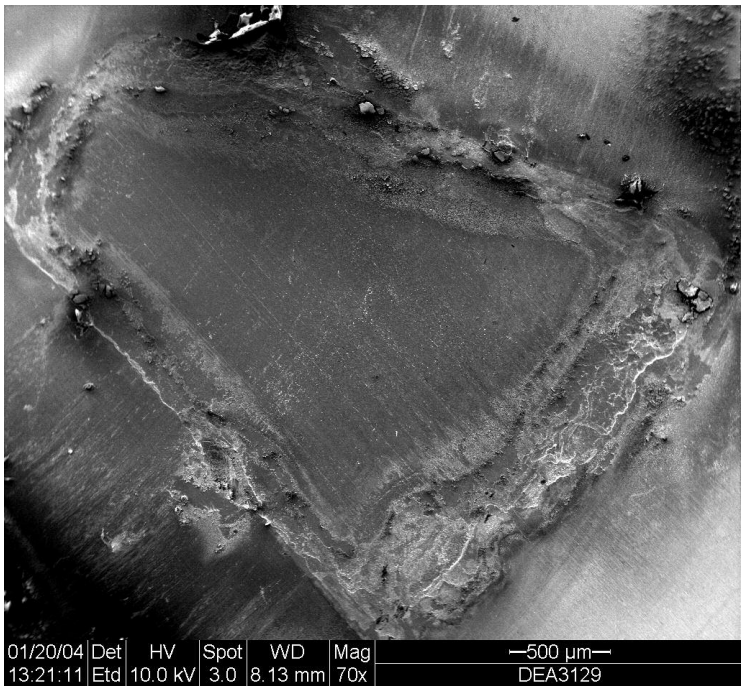

Figure 6: Crevice Corrosion formed under a Crevice Washer using CPP in 1 M NaCl at 90°C. Specimen DEA3129. The attack is deeper at the edges and does not progress horizontally.

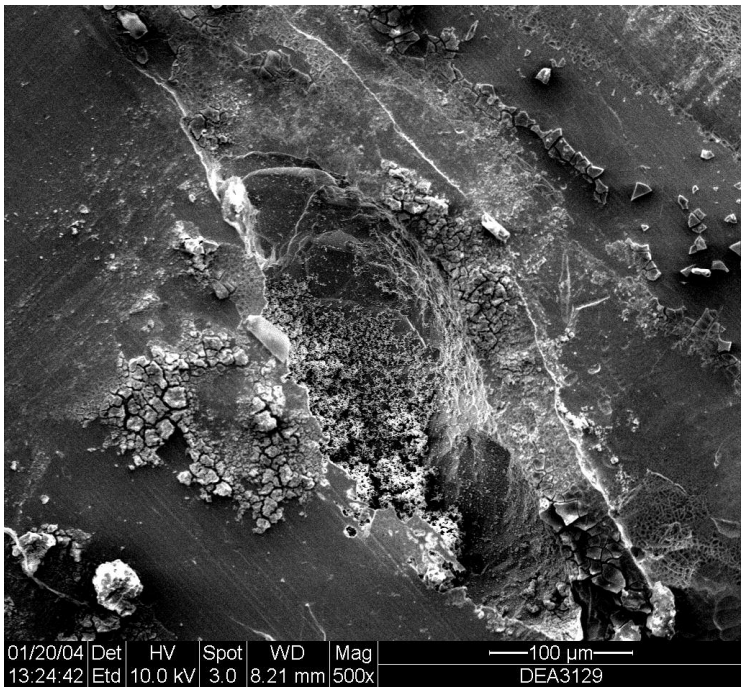

Figure 7: Detail of Crevice Corrosion formed under a Crevice Washer using CPP in 1 M NaCl at 90°C. Specimen DEA3129. The attack is deeper at the edges and does not progress horizontally.

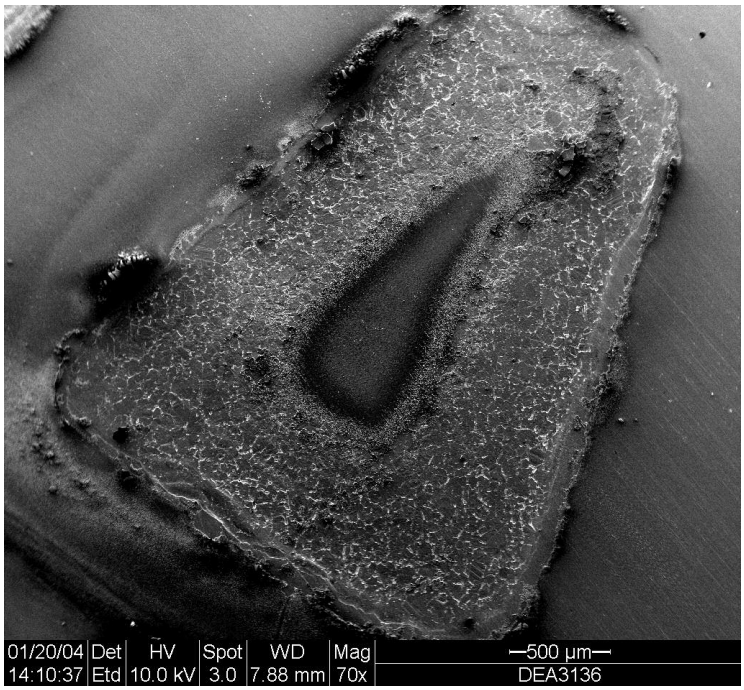

Figure 8: Crevice Corrosion formed under a Crevice Washer using THE in 1 M NaCl at 90°C. Specimen DEA3136. The attack is uniform in depth and progressed almost fully horizontally.

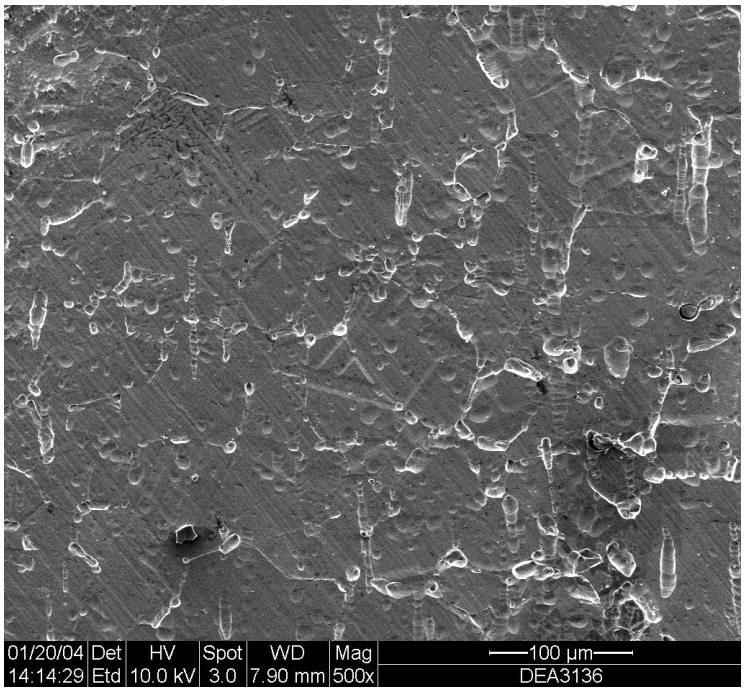

Figure 9: Detail of Crevice Corrosion formed under a Crevice Washer using THE in 1 M NaCl at 90°C. Specimen DEA3136. The attack is uniform in depth and progressed almost fully horizontally.

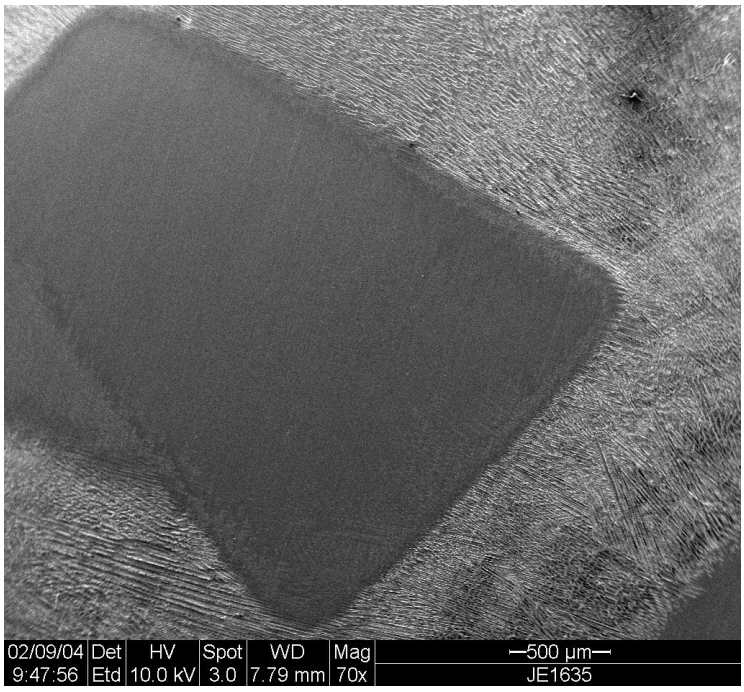

Figure 10: Localized Corrosion formed outside the Crevice Washer using CPP in 5 M $CaCl_2$ at 90°C. Specimen JE1635. The attack starts at the washer-metal interface and progresses outwards.

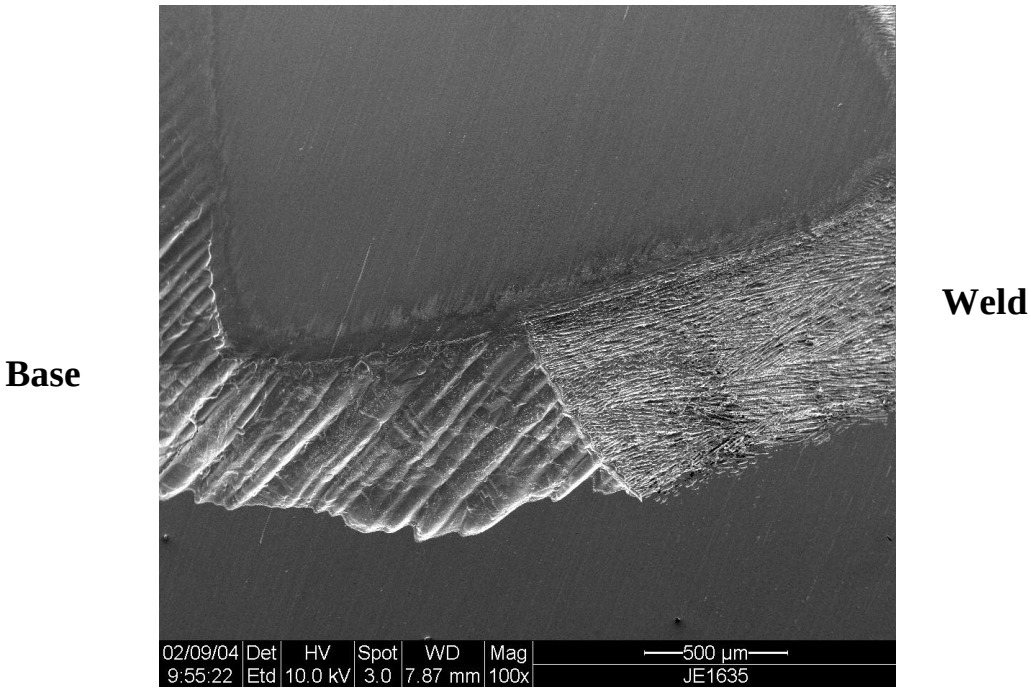

Figure 11: Localized Corrosion formed outside the Crevice Washer using CPP in 5 M $CaCl_2$ at 90°C. Specimen JE1635. The amount of attack is similar in the base metal (left) and in the weld seam (right).

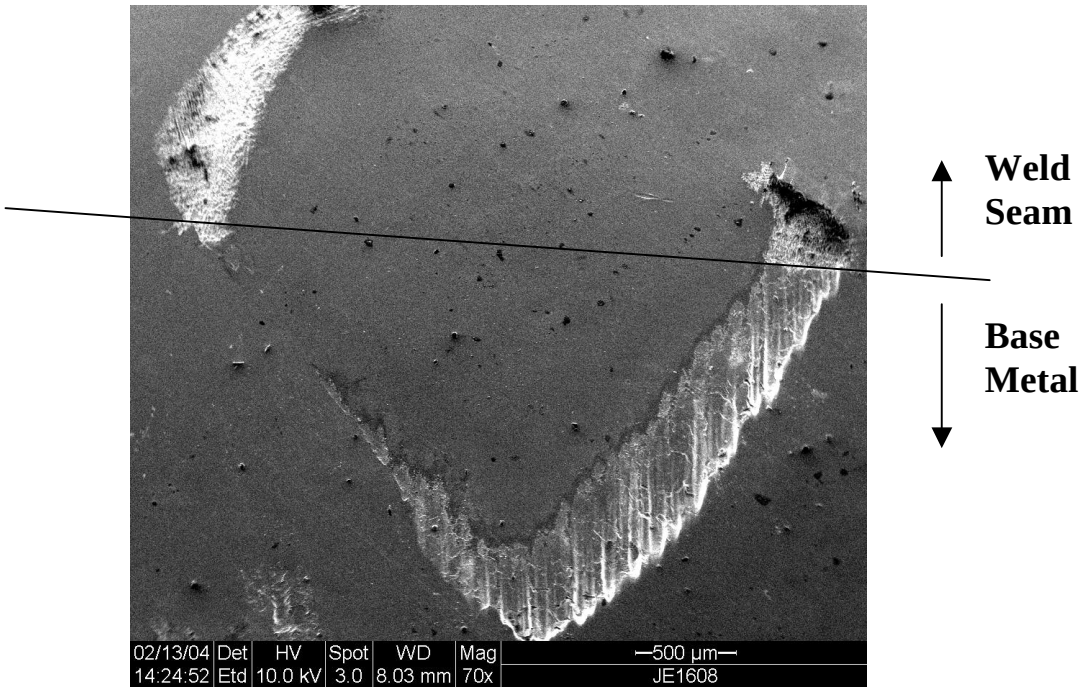

Figure 12: Crevice Corrosion formed under the Crevice Washer using THE in 5 M $CaCl_2$ at 90°C. Specimen JE1608. The attack is mostly in the base metal.

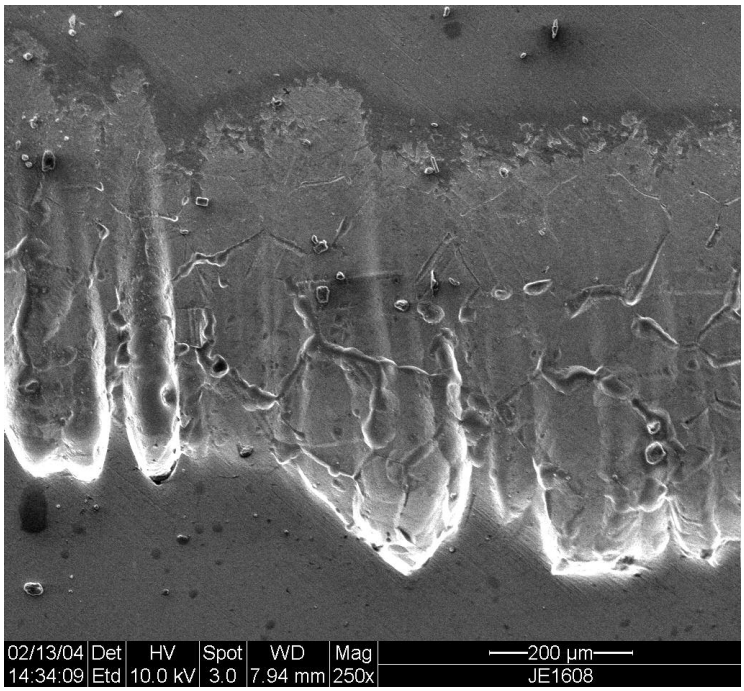

Figure 13: Crevice Corrosion formed under the Crevice Washer using THE in 5 M $CaCl_2$ at 90°C. Specimen JE1608. Intergranular attack in the crevice corrosion area. The attack is deeper in the edge of the crevice former and becomes shallower under the washer (top part of the picture).

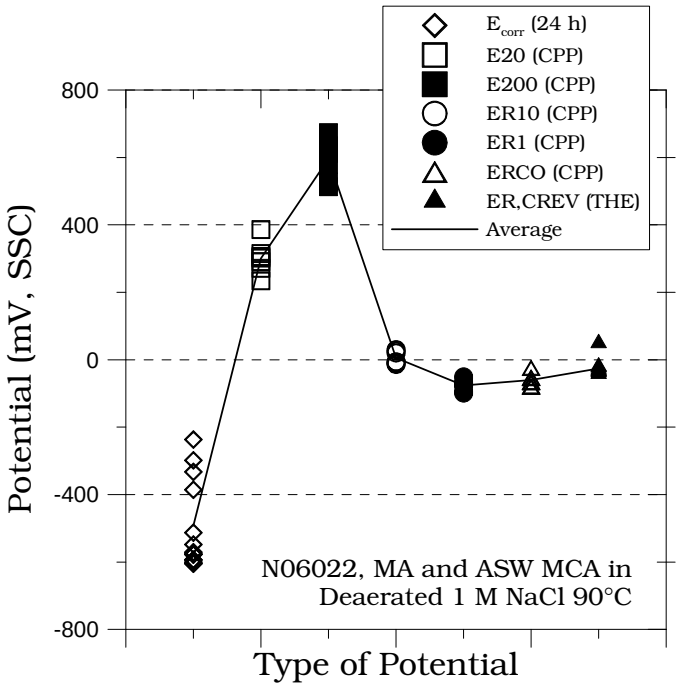

Figure 14: Parameters from Table 3 for CPP and THE tests in 1 M NaCl, 90°C.

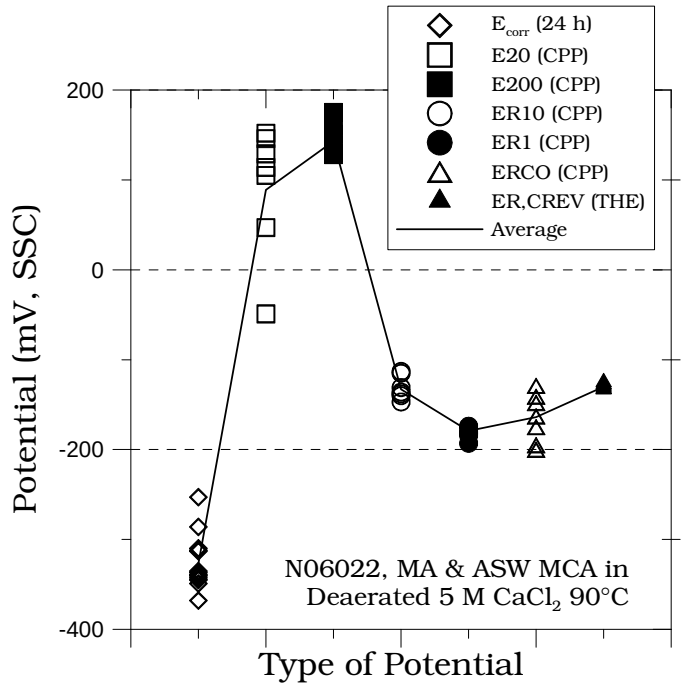

Figure 15: Parameters from Table 4 for CPP and THE tests in 5 M $CaCl_2$, 90°C.

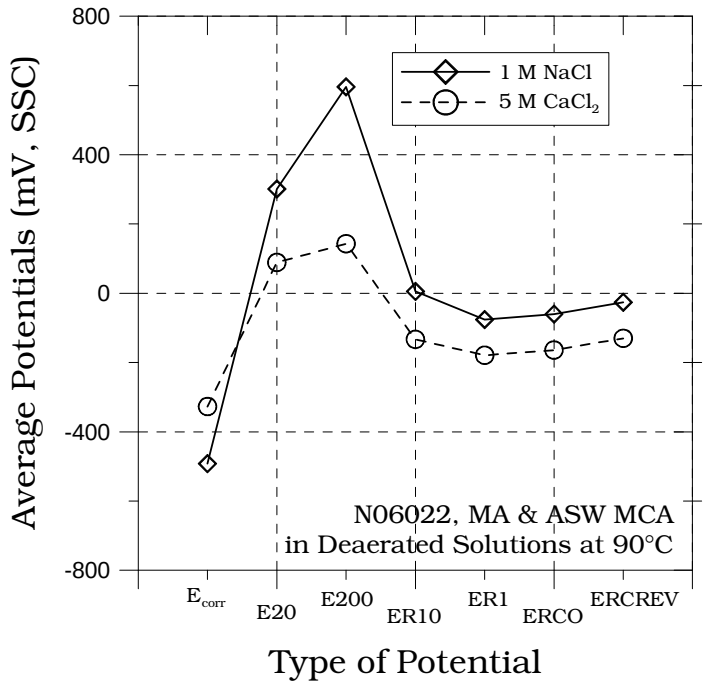

Figure 16: Comparison of Parameters for 1 M NaCl and 5 M $CaCl_2$, 90°C.